inter-noise 2008 From Silence to Harmony
37th International Congress and Exposition on Noise Control Engineering
26-29 October 2008·Shanghai·China

Active vibration control applied to a vacuum pump for high-precision equipment

A.P. Berkhoff[a,b], J.M. Wesselink[b], T.G.H. Basten[a]
[a] TNO Science and Industry, MON-Acoustics, PO Box 155, 2600AD Delft, The Netherlands,
[b] University of Twente, Faculty EEMCS, PO Box 217, 7500AE Enschede, The Netherlands

ABSTRACT

This paper presents results of a system for active vibration reduction on a setup with a vacuum pump that is tightly coupled with high-precision equipment. The precision of this equipment is critically dependent on the level of the vibrations that are introduced by the vacuum pump. The vibrations were reduced by a recently developed adaptive control scheme in a multi-input multi-output feedback configuration using a sampling rate of 12 kHz. The convergence properties of this algorithm allowed effective tracking of the varying excitation spectrum. Programmable digital minimum-phase reconstruction and anti-aliasing filters at a sampling rate of 100 kHz were used for an optimal tradeoff between sampling errors and phase shift. Effective broadband control was obtained in the frequency range of 100 Hz to 5 kHz, leading to 11.3 dB average broadband reduction on the error sensors.

1 INTRODUCTION

Increased accuracy demands in high-precision equipment make disturbing vibrations more and more important. In the application at hand, a turbomolecular vacuum pump is the disturbing vibration source. These pumps are applied in precision equipment applications where high vacuum is required, such as electron microscopes. Generally, the pumps are connected close to the vacuum vessel because the attainable vacuum level decreases drastically with increasing distance. Moreover, the static forces due to the pressure difference between the inner and outer side of the system make it difficult to apply soft connections between pump and the vessel. Passive vibration isolation, which is based on an impedance mismatch, implies using a soft connection between the pump and the vessel. Therefore, passive isolation methods based on soft connections are not regarded as the most appropriate means to isolate the vibration between the pump and the vessel. In this paper an active approach for reducing the vibration is considered, which allows the use of stiff connections between the pump and the vessel. In Ref. [1], a first attempt was described to realize such an active system. This attempt was based on tonal control using internal model control (IMC) for generating an independent reference signal. In ref. [1], the step to full broadband control was already anticipated. However, full broadband control based on the hardware and the algorithms described in Ref. [1] prevented the use of sufficiently high sample rates. A sample rate of 2 kHz could be obtained for broadband control, which was found to be too low to

[a] Email address: arthur.berkhoff@tno.nl

obtain meaningful vibration reductions at the relatively important high signal frequencies. In the experiments described in Ref. [5], the more powerful and compact control hardware of Ref. [2] was used, as well as the algorithm from Ref. [3], having increased convergence speed and better efficiency. The section on the experimental results in this paper will demonstrate the increase of performance as compared to the previous system of [1].

2 METHODS

The test setup including the turbomolecular vacuum pump, the actuators and the sensors is shown in Figs. 1 to 4. As mentioned in Ref [1], the main excitation direction of the vacuum pump is the vertical direction. Therefore, the excitation forces of the actuators were also in the vertical direction. Three electromagnetic proof-mass actuators of type Motran IFX 20-100 were used generating the control forces. Three Endevco M50 accelerometers were used for measurement of the acceleration in the vertical direction.

For this application, a fully coupled multiple-input multiple-output control algorithm was required. The particular algorithm that was used is able to use multiple reference signals in an efficient way [2,3]. The algorithm has been termed regularized modified filtered-error algorithm [3]. The algorithm uses preconditioning in combination with a double set of control filters in order to eliminate adverse effects on convergence of phase distortion and delays in the adaptation loop [3]. Such an implementation is made possible by using a state-space based description of relevant transfer functions, for which efficient and robust decomposition techniques exist. Regularization has been implemented in various parts of the algorithm, with the most important being the generalized effort weighting [3]. The algorithm has a number of advantages as compared to the standard filtered-error algorithm [4], such as considerably improved convergence speed, improved stability and robustness, a reduced computational complexity, and, for some applications, improved noise reductions. A disadvantage is that the complexity to program the algorithm is considerably higher. Nevertheless, the algorithm has been implemented successfully for both feedforward and feedback configurations.

The basis of the hardware for the control system is an Intel Mobile processor with an RT-Linux operating system (Fig. 5). Real-time code for this platform is generated using Matlab and Simulink. The control system has 16 analog inputs and 16 analog outputs. The sampling rate is nominally 100 kHz. Multi-stage decimators and multistage interpolators are implemented on FPGA in order to realize lower sample rates. This hardware allows to set the desired sample rate, but also the desired compromise between reconstruction errors, sampling errors, and phase distortion of the control loop, since the coefficients of the interpolation filters and decimation filters are fully programmable.

The algorithm minimizes the variance of the error signals using a feedback architecture based on Internal Model Control (IMC). The sample rate was set to 12 kHz and the order of the identified state-space model to 80. The controller had 100 coefficients for each actuator-sensor combination, resulting in a total of 900 controller coefficients. The length of the all-pass part of the transfer function was 150 samples. The regularization was based on the mean-square value of the control signals. The magnitude of the pertinent transfer function responsible for the regularization was set to approximately 40 dB below the maximum of the transfer function for the secondary path; eventually, the value for regularization was chosen to be -20 dB.

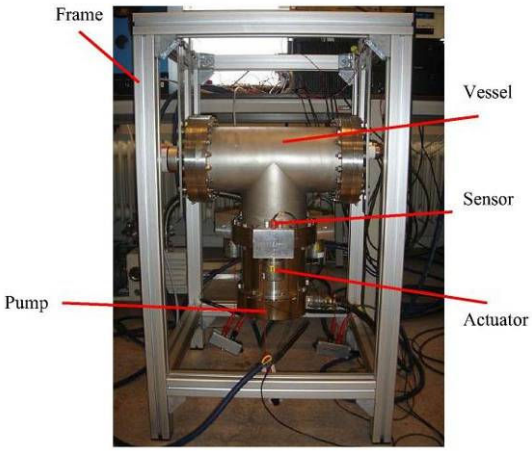

Figure 1. Experimental setup.

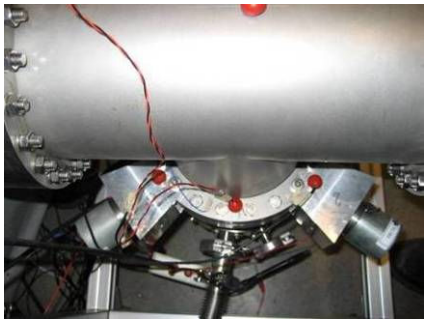

Figure 2. Experimental setup as seen from above (front).

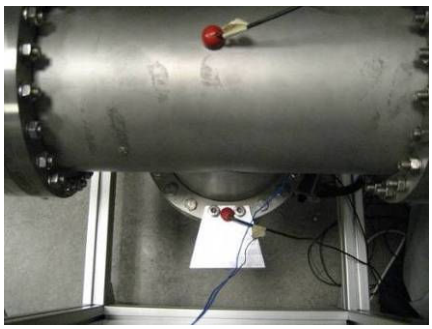

Figure 3. Experimental setup as seen from above (rear).

Figure 4. Experimental setup (side view) showing the 3 actuators for the vertical direction and 2 actuators for the horizontal direction.

Figure 5. InMAR Control hardware with 16 analog inputs and 16 analog outputs based on an Intel Mobile processor and FPGA.

3 EXPERIMENTAL RESULTS

Figs. 6 and 7 show the results of the system identification for a model order of 80. The variance accounted (VAF) was 97%. The magnitude of the frequency response function is shown in Fig. 6 and the phase is shown in Fig. 7. At frequencies below 1 kHz the system is not diagonally dominant and a strong cross-coupling between the actuator-sensor pairs exists. For frequencies above 1 kHz, the system is diagonally dominant. However, in this frequency range, the phase of the transfer function is considerably higher than 180 degrees which would make low-order collocated feedback control for this setup rather ineffective. The secondary path between actuator 1 and sensor 1 is shown in Figs. 8 to 10, which subsequently are the transfer function magnitude, the transfer function phase and the impulse response. The algorithm as used in this paper [3] is based on a decomposition of the multichannel transfer function in a multichannel minimum-phase factor and a multichannel all-pass factor by so-called inner-outer factorization. In order to ensure stability of the system when an inverse of the minimum-phase factor is used, the minimum-phase factor is determined after a regularizing augmentation of the secondary path, which in this case consists of a simple diagonal gain matrix. The resulting regularized minimum-phase factor (i.e., outer-factor) between actuator 1 and sensor 1 is shown in Figs. 11 to 13, which subsequently are the transfer function magnitude, the transfer function phase, and the impulse response. Fig. 14 shows the transfer function magnitude between actuator 1 and sensor 1 of the inverse outer-factor, and Fig. 15 displays the corresponding impulse response. Fig. 16 shows the transfer function magnitude between actuator 1 and sensor 1 of the all-pass factor (inner factor).

The result of the control system for the three error sensors is given in Fig. 17. The broadband reduction on the three error sensors is 13.4 dB, 10.0 dB and 10.8 dB. The reduction on the basis of the sum of the powers of the three sensor signals is 11.3 dB. On some peaks, such as around 800 Hz, the reduction is 20 dB to more than 30 dB. It can also be seen that the controller not only reduces harmonic components in the vibration spectrum, but also the broadband part of the spectrum, as can be seen in the frequency range of 400 Hz to 600 Hz (sensor 2 and 3), around 1.6 kHz (all three sensors), and around 4 kHz. From the experiments it became clear that the spectrum was not constant but rather time-varying. Therefore, the use of an adaptive algorithm proved to be useful. The rapid convergence of the algorithm allowed effective tracking of the time-varying vibration signals. Tests with a slower adaptation speed resulted in higher residual levels, i.e. lower reductions, also after convergence during a rather long time (hours). Therefore, the rapid adaptation of the control algorithm proved to be especially useful for this application.

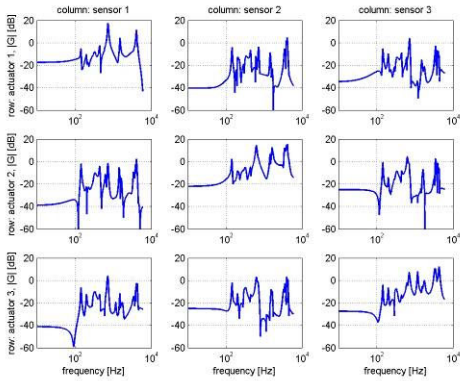

Figure 6. Magnitude of the transfer function between the actuators and the error sensors.

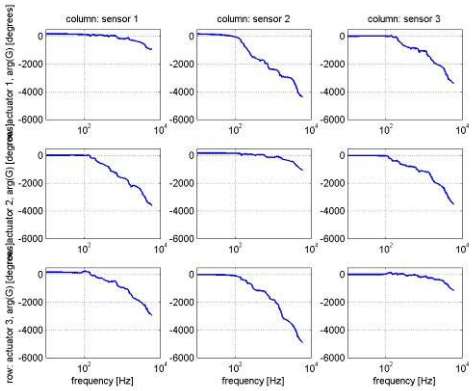

Figure 7. As Fig. 6, phase response.

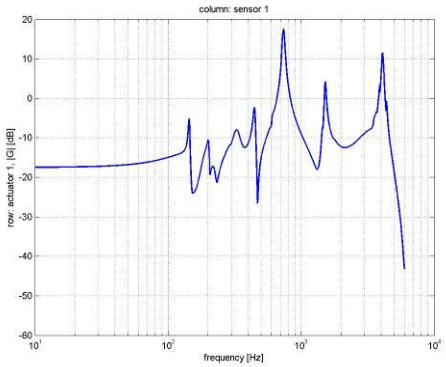

Figure 8. Secondary path transfer function magnitude (actuator 1, sensor 1).

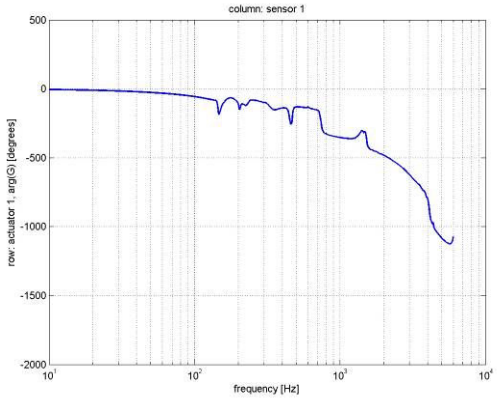

Figure 9. Secondary path transfer function phase (actuator 1, sensor 1).

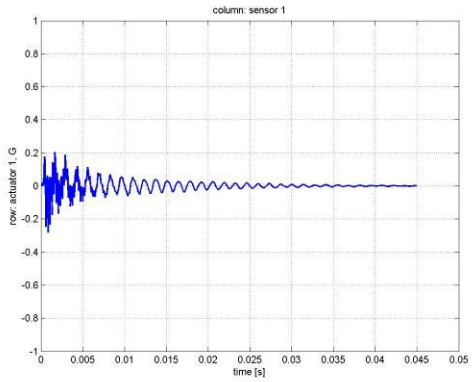

Figure 10. Secondary path impulse response (actuator 1, sensor 1).

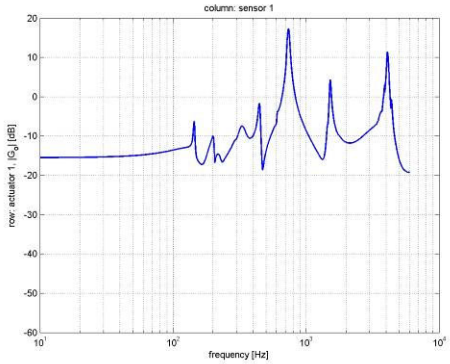

Figure 11. Regularized secondary path minimum-phase transfer function magnitude (actuator 1, sensor 1).

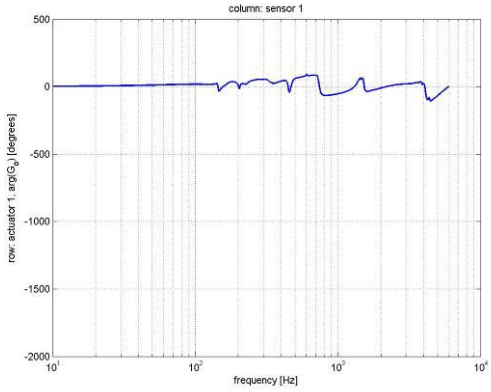

Figure 12. Regularized secondary path minimum-phase transfer function phase (actuator 1, sensor 1).

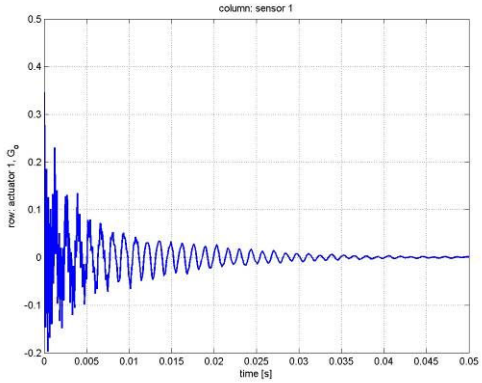

Figure 13. Regularized secondary path minimum-phase impulse response (actuator 1, sensor 1).

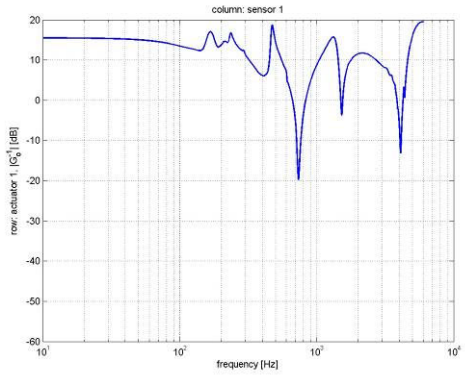

Figure 14. Regularized secondary path minimum-phase inverse transfer function magnitude (actuator 1, sensor 1).

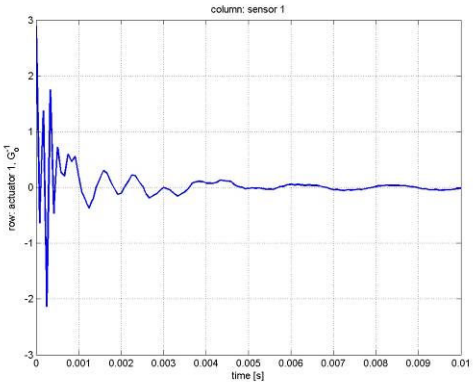

Figure 15. Regularized secondary path minimum-phase inverse impulse response (actuator 1, sensor 1).

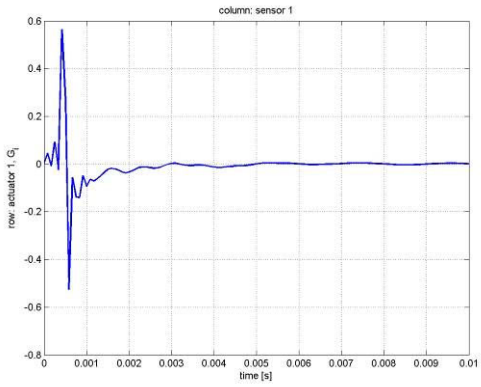

Figure 16. Regularized secondary path all-pass impulse response (actuator 1, sensor 1).

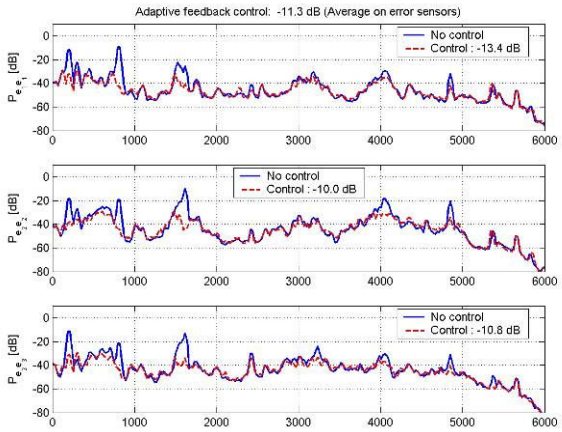

Figure 17. Spectra of the sensor signals, without control and with control using an adaptive feedback algorithm based on Ref. [3].

4 CONCLUSIONS

Adaptive broadband MIMO vibration control has been implemented for a turbomolecular vacuum pump at a sample rate of 12 kHz. The control system resulted in a broadband reduction of 11.3 dB for frequencies between 100 Hz and 5 kHz. Adaptive control was found to be necessary because of the rapidly varying disturbance spectrum.

5 ACKNOWLEDGEMENTS

The research and development related to the algorithm, the hardware and the software for the control system has been partly funded by the EU-6th framework project Intelligent Materials for Active Noise Reduction (InMAR). The research and development related to the setup for the turbo pump and application of the control system for this setup has been supported by the Innovation-oriented Research Program (IOP) Precision Technology, which is carried out by SenterNovem by order the Dutch Ministry of Economic Affairs.

6 REFERENCES

[1] T.G.H. Basten et al., Active vibration isolation of a rigidly mounted turbo pump, in *proc. ICSV13*, pp. 1-8, Eds. J. Eberhardsteiner, H.A. Mang and H. Waubke, International Institute of Acoustics and Vibration, 2006, presented at the 13th International Conference of Sound and Vibration, Vienna, Austria, July 2-6, 2006.

[2] A.P. Berkhoff and J.M. Wesselink, Multichannel Active Noise Control Systems and Algorithms for Reduction of Broadband Noise, *Proc. Adaptronic Congress 2007*, 23-24 May 2007, Göttingen, pp. 1-4, Adaptronic Congress Veranstaltung GbR, Göttingen, 2007.

[3] A.P. Berkhoff and G. Nijsse, A rapidly converging filtered-error algorithm for multichannel active noise control, *International Journal of Adaptive Control and Signal Processing* **21**(7), pp. 556-569, 2007.

[4] E.A. Wan, Adjoint LMS: an efficient alternative to the filtered-X LMS and multiple error LMS algorithms, Proc. ICASSP96, pp. 1842-1845, IEEE, 1996. Presented at the International Conference of Acoustics Speech and Signal processing, Atlanta, 1996.

[5] A.P. Berkhoff, J.M. Wesselink and T.G.H. Basten, Adaptive reduction of the vibrations from a vacuum pump for high-precision equipment, *Proc. Adaptronic Congress 2008*, 20-21 May 2008, Berlin, pp. 1-4, Adaptronic Congress Veranstaltung GbR, Göttingen, 2008.